Depth Dependent Microstructure of Ion-Irradiated Type 316 Stainless Steels

B. Sindelar, G.L. Kulcinski and R.A. Dodd

September 1983

UWFDM-552

Presented at the Third Topical Meeting on Fusion Reactor Materials, Albuquerque, NM, 19-23 September 1983] [J. Nucl. Matls. **122&123** (1984) 246.

FUSION TECHNOLOGY INSTITUTE

UNIVERSITY OF WISCONSIN

MADISON WISCONSIN

Depth Dependent Microstructure of Ion-Irradiated Type 316 Stainless Steels

B. Sindelar, G.L. Kulcinski and R.A. Dodd

Fusion Technology Institute
University of Wisconsin
1500 Engineering Drive
Madison, WI 53706

http://fti.neep.wisc.edu

September 1983

UWFDM-552

Presented at the Third Topical Meeting on Fusion Reactor Materials, Albuquerque, NM, 19-23 September 1983 [J. Nucl. Matls. **122&123** (1984) 246].

DEPTH DEPENDENT MICROSTRUCTURE IN ION-IRRADIATED 316 TYPE STEELS

R.L. SINDELAR, G.L. KULCINSKI, and R.A. DODD

Nuclear Engineering Department, University of Wisconsin, 1500 Johnson Drive, Madison, WI 53706

A cross-section technique was developed and employed to observe 14 MeV nickel-ion damage to Type 316 stainless steels. Solution-quenched 316 SS and the P-7 alloy were irradiated at a flux of 3 x 10^{11} Ni ions/cm^2/s to fluences up to 3.3 x 10^{16} Ni ions/cm^2. The heavy-ion irradiation of the P-7 at 650°C produced a unique damage state. A near-surface void-free zone was observed. In addition, a bi-modal void distribution was produced at the calculated peak of the damage distribution.

1. INTRODUCTION

The cross-section technique for observing heavy-ion radiation effects in metals has been shown to yield a large amount of information from a single irradiated sample.[1,2] Such studies have involved plating and jet-thinning for TEM analysis of similar metals. In the present study, a technique has been developed for examining austenitic Fe-Cr-Ni alloys. The present technique differs from previous procedures aimed at observing these alloys in cross section after light ion irradiations.[3,4] This technique has revealed features of the damage state never before observed. In particular 316 SS and the P-7 alloy (a high swelling "pure" 316 SS alloy[5-8,13-15]) were irradiated and observed in cross-section. The P-7 alloy was found to contain a bi-modal void distribution near the calculated peak damage region. The presence of oxygen at high levels in the P-7 alloy is suggested to be a factor in the development of the observed bi-modal void distribution.

2. EXPERIMENTAL PROCEDURE

Table 1 gives the composition of the annealed 316 SS (Fusion Program reference heat #15893) and the P-7 alloy used in this study. The 316 SS was thermomechanically prepared by T. Roche at Oak Ridge National Laboratory. The P-7 alloy was rolled to 0.5 mm (0.020 in) and then solution annealed for 1 hour at 1000°C (T/T_M = 0.75) in an argon atmosphere followed by a water quench. Pre-irradiation preparation of the P-7 alloy involved a mechanical polish with 0.3 μm alumina powder. The samples were not given a pre-irradiation electropolish to avoid the introduction of hydrogen into the metal that occurs when the sample is made anodic in the polish cell.[1]

Irradiations were performed at the University of Wisconsin Heavy-Ion Irradiation Facility using 14 MeV Ni^{3+} ions. Table 2 lists the fluence, flux and temperature parameters of the irradiations.

The cross-section technique developed for the post-irradiation TEM analysis of the depth dependent damage of heavy ions is described below. The form of the irradiated specimen is a 0.5 cm x 1.0 cm foil. The irradiated region of the foil was a 3 mm diameter circular area in the center of the foil. Following the irradiation, the specimens were lightly swabbed with a 0.3 μm alumina-water slurry to remove

*This research was sponsored by the Department of Energy. The authors would like to thank D.L. Plumton, H. Attaya and J. Billen for their assistance in this project.

Table 1
Composition of MFE Heat # 15893 316 SS and the "pure" 316 SS, P-7 Alloy

Material	Composition (wt.%)[a]										
	Cr	Ni	Mo	Mn	Si	C	P	S	Ti	O	W
316 SS	17.4	12.6	2.2	1.81	0.65	0.05	0.030	0.020	< 0.001	-	-
P-7 alloy	17	16.7	2.5	0.03	0.1	0.005	-	-	0.01	0.03*	0.068

[a] Balance Fe

* Oxygen determined before rolling and annealing

Table 2
Irradiation Conditions (14 MeV Nickel Ions); All Specimens Solution-Quenched Prior to Irradiation

Material	dpa at 1μm	peak dpa	Fluence (ions/cm^2)	Flux (ions/cm^2/s)	Temp.(°C)
1. 316 SS	3	12	1×10^{16}	3×10^{11}	575
2. P-7 alloy	1	5	0.33×10^{16}	3×10^{11}	650
3. P-7 alloy	10	50	3.3×10^{16}	3×10^{11}	650

the contamination caused by the breakdown of the residual hydrocarbons in the irradiation chamber. To insure a good bond with the nickel plating, the foil was made anodic in a solution consisting of 40 mℓ HCl, 60g $NiCl_2$,in 250 mℓ H_2O at room temperature. This solution is a modification of that used by Woods. The current density during the surface removal was 200 mA/cm^2, and the duration of the strike was 3 seconds. Interference microscopy reveals that less than 100 nm was removed from the foil surface during this step. Next the polarity was reversed and the foil plated in this bath for 5 minutes before being transferred into the plating bath. The plating bath consisted of 150g $NiSO_4$, 150g $NiCl_2$, and 70g boric acid in 1000 mℓ H_2O at 75°C. The partially plated foil was made anodic in this plate bath at a current density of 200 mA/cm^2 for about 15 seconds. The polarity was then reversed and the foil plated for ~ 36 hours. During the plating period, a fine stream of N_2 gas bubbles was allowed to flow over the surface of the foil thereby washing away the H_2 bubbles formed by electrolysis. These bubbles otherwise cause porosity in the plating.

After the plating step, the sample was sliced into 250 μm (~ 0.010 in) thick sections normal to the irradiated surface and a 3 mm disc was cut from a slice containing the irradiated region.[1] This disc was then thinned for TEM observation using a two-step jet-thinning technique. First the disc was twin-jet polished in a 30% HNO_3, 70% methanol solution at -20°C and a 10 volt potential for 3 minutes. This solution preferentially polished the nickel plating. The next step involved twin-jet thinning to perforation in an electrolyte containing 10% $HClO_4$, 90% CH_3COOH, with 20g/ℓ CrO_3, and 10g/ℓ $NiCl_2$ at room temperature and a potential of 40 volts. A small diameter (0.7 mm) tantalum aperture was placed over the disc during the first 30 seconds of polish to obtain a region of enhanced polish at the steel-nickel interface. This second solution preferentially thins the steel. The above procedure causes perforation of the disc at the interface region, thereby producing a specimen suitable for TEM analysis. In this study TEM analysis was performed on a JEOL JEM-200CX electron microscope.

3. RESULTS

The irradiated 316 SS specimen (see Table 2), observed in cross-section revealed a dislocation network of density ~ 10^{11} cm^{-2} extending from the surface into the foil a distance of approximately 3 μm. This corresponds to the calculated range[9] of the displacement damage of 14 MeV Ni incident on 316 SS. No voids or precipitates were detected under TEM analysis for the 316 SS sample irradiated to a peak dose of 12 dpa. Other studies with Ni ions at this temperature show voids present at a slightly higher dose.[10]

The P-7 alloy, when irradiated at the conditions in Table 2, was found to contain a bi-modal void distribution near the calculated peak of the damage distribution (see Fig. 1). Figure 2 shows a TEM micrograph of this alloy irradiated to a peak level of 50 dpa at 650°C. The larger voids present in Fig. 2 approach the value of the foil thickness in this region (200 nm). Many of these voids intersect the foil surface. Stereo microscopy analysis in thicker regions of the foil revealed that these features are not a polishing artifact and were once completely contained in the foil. Also evident in Fig. 2 is a denuded zone extending over 0.5 μm from the foil surface. This is consistent with the HVEM data on surface effects in stainless steels irradiated at high temperatures.[11]

Figures 3, 4, and 5 are plots of the average void diameter, number density, and swelling as a function of depth from the original foil surface. A classification labeling voids > 100 nm as "large voids" and voids < 100 nm as "small voids" was used in construction of the plots. This bi-modal distribution was already established in the low-fluence (1dpa at 1μm) P-7 alloy. Results of the analysis of this alloy are listed in Table 3.

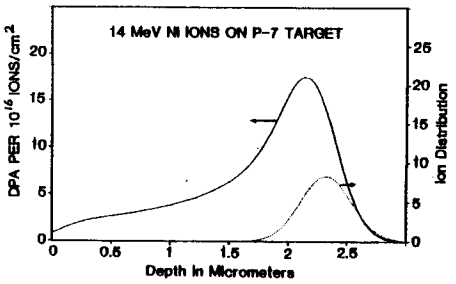

FIGURE 1
Damage level calculated as a function of depth from the incident irradiated surface using the Brice[12] code.

4. DISCUSSION

Two interesting features were observed in this experiment. The first is the occurrence of a denuded zone at the foil surface. The second is the existence of a bi-modal void distribution near the calculated peak of the damage in the P-7 alloy.

The reasons for the decreasing denuded zone width probably can be associated with the increased damage level. The incubation dose for void formation in ion bombarded P-7 alloys is in the range of ~ 1 dpa. This level of damage is not reached until ~ 1 micron in the 3.3 x 10^{15} ion/cm^2 sample whereas the 1 dpa level is exceeded over the entire damage zone for the 3.3 x 10^{16} ion/cm^2 sample. The fact that the denuded zone is still ~ 0.6 μm in the higher fluence sample is attributed to the diffusion of defects to the free surface. Garner and Thomas[11] have shown in HVEM studies that a 0.6 μm void free zone exists at a dose of 6 dpa in 316 SS at 650°C.

The occurrence of a bi-modal void distribution has not been observed in a heavy-ion irradiated single phase material in the absence of injected or transmutated gas. A distinguishing feature of the P-7 alloy that may be responsible for the development of the observed bi-modal distribution is the high

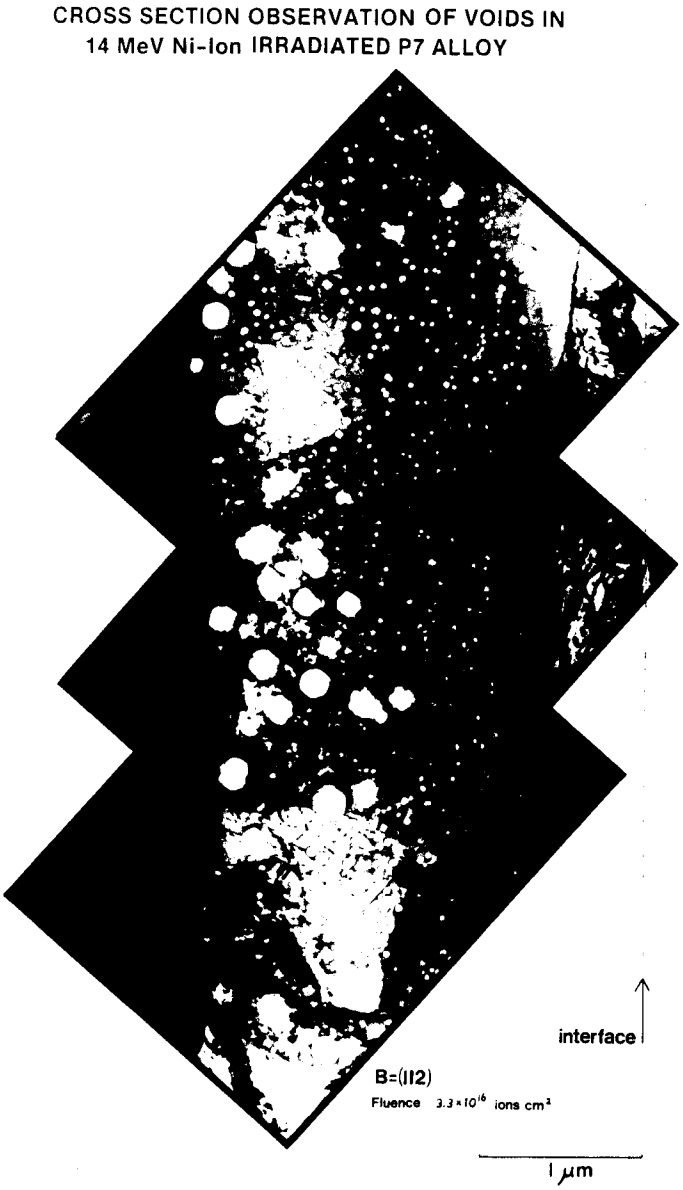

FIGURE 2
TEM micrograph showing a surface denuded zone and bi-modal void distribution in the peak damage region. The temperature of irradiation was 650°C.

Table 3
Comparison of the Low Fluence and High Fluence P-7 Alloys Irradiated at 650°C

Ion Fluence cm^{-2}	dpa at 1 μm	dpa at 2.25 μm	Large size void diam. at ~ 2.25 μm	Small size void diam. at ~ 2.25 μm	Surface Denuded Zone Width
3.3×10^{15}	~ 1	~ 5	101 ± 20 nm	34 ± 15 nm	0.9 ± 0.2 μm
3.3×10^{16}	~ 10	~ 50	195 ± 15 nm	30 ± 10 nm	0.6 ± 0.1 μm

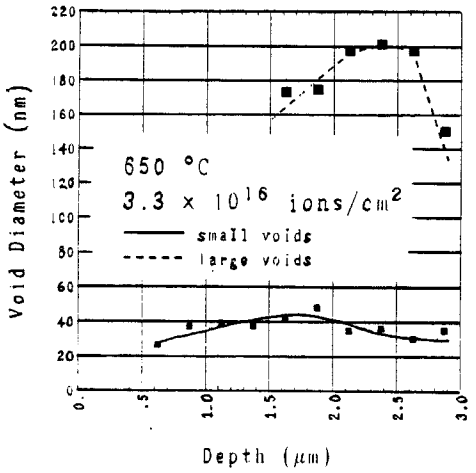

FIGURE 3
Average void diameter as a function of depth for the large size class voids and the small size class voids (see text). Note the decline of the average diameter of the small size class as the large size class appears at ~ 2.0 μm.

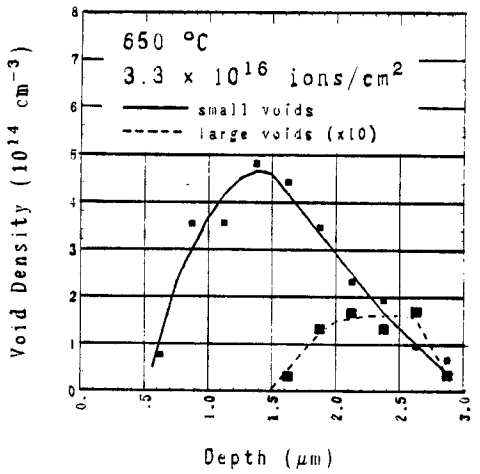

FIGURE 4
Void density as a function of depth for the two size classes of voids. Note the small (~ 1 x 10^{13} cm^{-3}) void density of the large size class.

oxygen content of the material (Table 1). In addition to the content stated in Table 1, oxygen may have been introduced during the 1 hour, 1000°C argon-atmosphere solution-quench. An oxide coating was removed from the sample after the treatment indicating some oxygen in the atmosphere of the furnace. This may increase the oxygen content over the reported 0.03 wt.% (1000 at.ppm).

Oxygen is readily chemisorbed on clean free surfaces for many metals.[16] This phenomenon may affect void evolution by lowering the surface energy of a void which could thereby reduce the tendency for voids to emit vacancies. In addition, oxygen may affect the evolution of a void by combining with other elements at the void surface to form a "void coating".[17] A void coating is suggested to create a defect-void image interaction and thereby bias the void against interstitial capture.

Voids forming early in the irradiation may provide a free-surface sink for the oxygen in the surrounding matrix. These voids would then have their growth kinetics altered by the oxygen. Voids forming at a later irradiation time would be affected less due to the reduced

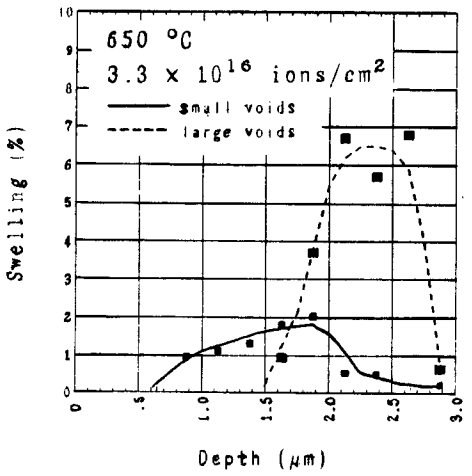

FIGURE 5
Cavity-induced swelling (ΔV/V) as a function of depth for the two size classes of voids. The peak swelling (~ 6.5%) occurred at the calculated peak damage level of ~ 50 dpa.

matrix oxygen level.

For the bi-modal distribution to be seen only at depths greater than 1.75 μm, it possible that the oxygen is removed from the near surface region by high temperature diffusion and/or radiation-induced diffusion to the foil surface. A thermal diffusion calculation using oxygen in γ iron ($D = 1.6 \times 10^{-9}$ cm^2/sec at 650°C[18]) indicates that up to 90% of the oxygen initially present at a depth of 1 μm could leave the sample during the 5 minutes prior to irradiation when the sample was at 650°C. However, such diffusion calculations do not consider the effect of Cr which might considerably reduce the oxygen diffusivity. Future analyses of the residual oxygen content may reveal the role that the thermal/radiation induced diffusivity has on the distribution of oxygen in the near surface region.

REFERENCES

1. J.B. Whitley, G.L. Kulcinski, P. Wilkes, H.V. Smith Jr., J. Nuc. Matl. 79 (1979) 159-169.

2. R.W. Knoll, P. Wilkes, G.L. Kulcinski, Phase Stability During Irradiation, Conf. Proceedings of the Metallurgical Society of AIME, Oct. 5-9, 1980, 123.

3. R.A. Spurling, C.G. Rhodes, J. Nuc. Matl. 44 (1972) 341-344.

4. K. Shiraishi et al., ASTM STP 782 p. 927-940.

5. K. Farrell, N.H. Packan, J. Nuc. Matl. 85 & 86 (1979) 683-687.

6. N.H. Packan, K. Farrell, J. Nuc. Matl. 85 & 86 (1979) 677-681.

7. K. Miyahara, N.H. Packan, N. Igata, Effects of Radiation on Materials: Eleventh Conference, ASTM STP 782 (1982) 941-952.

8. H.R. Brager, F.A. Garner, Effects of Radiation on Materials, Eleventh Conf., ASTM STP 782 (1982) 152-165.

9. I. Manning, G.P. Mueller, Computer Physics Comm. 7 (1974) 639-650.

10. J.A. Hudson, J. Nuc. Matl. 60 (1976) 89.

11. F.A. Garner, L.E. Thomas, Effects of Radiation on Substructure and Mechanical Properties of Metals and Alloys, ASTM STP 529 (1973) 303-325.

12. D.K. Brice, "Ion Implantation Range and Energy Deposition Codes COREL, RASE4 and DAMG2," SAND 77-0622 (1977).

13. N.H. Packan, J. Nuc. Matl. 103 & 104 (1981) 1029.

14. W.G. Johnston, T. Lauritzen, J.H. Rosoloksi, A.M. Turkalo, "The Effect of Metallurgical Variables on Void Swelling", General Elecric Report 76CRD010, Jan. 1976.

15. J.M. Leitmaker, E.E. Bloom, J.O. Stiegler, J. Nuc. Matl. 49 (1973) 57-66.

16. K. Tanaka, K. Tamaru, J. of Catalysis 2 (1963) 366.

17. W.G. Wolfer, L.K. Mansur, J.A. Sprague, in Radiation Effects in Breeder Reactor Structural Materials (1977) 841.

18. J.H. Swisher, E.T. Turkdogan, Trans. Met. Soc. AIME 239 (1967) 426-431.